**Western Kentucky University**
## TopSCHOLAR®

Honors College Capstone Experience/Thesis Projects

Honors College at WKU

Spring 5-2012

# Using Two Different Approaches for the Creation of Poly(3-Hexylthiophene)-Functionalized Siloxane Nanoparticles for Organic-Based Solar Cells

Nicholas A. Wright
*Western Kentucky University*, nicholas.wright999@topper.wku.edu

Follow this and additional works at: http://digitalcommons.wku.edu/stu_hon_theses

Part of the Organic Chemistry Commons, and the Physical Chemistry Commons

USING TWO DIFFERENT APPROACHES FOR THE CREATION OF

POLY(3-HEXYLTHIOPHENE)-FUNCTIONALIZED SILOXANE NANOPARTICLES

FOR ORGANIC-BASED SOLAR CELLS


A Capstone Experience/Thesis Project

Presented in Partial Fulfillment of the Requirements for

the Degree of Bachelor of Science with

Honors College Graduate Distinction at Western Kentucky University


By

Nicholas Aigner Wright

\*\*\*\*\*




Western Kentucky University
2012




CE/T Committee:

                                              Approved by

Professor Hemali Rathnayake, Advisor

Professor Lester L. Pesterfield

                                       _____

Professor Justin Litke                          Advisor
                                             Department of Chemistry

ABSTRACT

Poly(3-hexylthiophene)-functionalized silsesquioxane nanoparticles were prepared from direct hydrolysis and condensation of P3HT-silane precursor using "grafting from" and "grafting to" methods. The size, shape, and surface morphology of these polymer grafts particles were visualized using transmission electron microscopy and scanning electron microscopy. Their compositions confirmed by FTIR, thermogravimetric analysis and elemental analysis. The XRD analysis revealed the polymer orientation and packing pattern of the nanocomposites, indicating the highly ordered lamella stacks of P3HT polymer chains. The photovoltaic performance of the blends of P3HT-nanohybrid with the C60 derivative PCBM was evaluated upon annealation in different temperatures, ranging from 50°C to 150 °C. The power conversion efficiency of the best test device was 2.46% (3.8%) for the device configuration of ITO/PEDOT:PSS/P3HT-NPs:PCBM/LiF/Al.

Keywords: P3HT, OPVs, Solar Cells, Siloxanes, Photovoltaics, Nanocomposites.

Dedicated to my friends and family for always being there for me and for helping me get his far in life.  Thank you.

ACKNOWLEDGMENTS

VITA

December 18, 1988............Born – Wilmington, Delaware

2007..................................Berea Community High School, Berea, Kentucky

2010..................................Became an ACS Member

2010, 2011.........................Louis Stokes Alliance of Minority Participation Recipient

2011..................................Kentucky Academy of Sciences, Poster Presentation, $1^{st}$ Place

2012..................................ACS National Meeting, San Diego, Poster Presentations

2012..................................Kentucky Nanotechnology Symposium, Poster Presentation

2012..................................National Science Foundation Graduate Research Fellowship Recipient

2012..................................Accepted into Vanderbilt Graduate Research Program


Publications

Nicholas Wright, Amar Patel, Jenna Binion, and Hemali Rathnayake. "Poly(3-hexykthiophene)-functionalized Siloxane Nanoparticles for Organic-based Solar Cells." *Polymeric Materials Science & Engineering* **2012**, 106, 431.

Nicholas Wright, Amar Patel, Jenna Binion Debra Jo Scardino, Nathan I. Hammer, and Hemali Rathnayake, "Poly(thiophene) functionalized ormosils for Organic based solar cells." *Chem. Mater.* **2012**, *Submitted*.


Fields of Study

Major Field: ACS Chemistry

Minor Field: Mathematics

TABLE OF CONTENTS

LIST OF FIGURES

LIST OF SCHEMES

# LIST OF TABLES

CHAPTER 1

INTRODUCTION

Several different attempts, such as artificial photosynthesis, have been made to

create photovoltaic devices that can mimic the photosynthetic process of plants.

Attempts have been made to create materials that use the photovoltaic effect, the creation

of voltage or electric current in a material upon exposure to light.  The photovoltaic effect

is very similar to the photoelectric effect but differs in process.  In the photoelectric

effect, electrons are emitted from the surface of a material due to the absorption of

electromagnetic radiation.  In the photovoltaic effect, electrons are transferred from the

valance band to the conduction band within a given material, resulting in the buildup of

voltage between two electrodes.[1]  Some of these attempts have been successful and have

been commercialized, however these devices are not inexpensive by any means.  For

example, using 41,000 square inches of silicon based solar panels on the roof of a

"typical home" in America would cost about $16,000 to yield about 350 milliwatt hours

per day.[2] This is assuming that the sun has a maximum exposure time of 5 hours to the

solar panel when the panels are generating their maximum power.  This cost then doubles

for extra equipment for when the sun is not shinning.  This brings the cost to $32,000

before use.[2] This cost far exceeds the typical American's expendable income.

Due to the fundamental interest in the photophysics and photochemistry of

excited states in organic molecules, this is gives reason as to why photo-induced electron

transfer has been so extensively investigated.  Obtaining the right configuration of

organic molecules and the theories found in physical chemistry pertaining to photo

induced effects, a cost effective device could be created to aid in solving the impending

energy crisis.

Within this literature review several aspects of organic-based photovoltaics will

be discussed under two main categories: Organic photovoltaic cells and improving

organic photovoltaics.  Within the first category, information pertaining to what organic

photovoltaic cells are and the different types of OPVs will be given.  In the second

category, information covering the performance measures, Factors, and Equation will be

shown, as well as the incorporation of poly-(3-hexylthiophene) (P3HT) silsesquioxane

(SSQ) nanoparticles (NP) in organic photovoltaic (OPV) cells.

## I. Organic Photovoltaic Cells

*What Are OPVs*

As introduced earlier, a photovoltaic device could help to solve an impending

energy crisis cost efficiently.  OPVs are a combination of organic materials and

photovoltaic cells.  An organic photovoltaic cell is a specialized semiconductor diode that

converts visible light into direct current (DC) electricity.  Some OPVs can also convert

infrared (IR) and/or ultraviolet (UV) radiation into DC as well.[3] A common characteristic

of both the small molecules and polymers used in OPVs is they all have large conjugated

systems.  A conjugated system is usually created when carbon atoms are covalently

bonded to one another alternating in single and double bonds to each other, this can also

be seen as the chemical reactions of hydrocarbons. The hydrocarbons' electrons, in the $p_z$

orbitals, delocalize and form a delocalized bonding $\pi$ orbital and a $\pi^*$ antibonding orbital.

The delocalized $\pi$ orbital is the highest occupied molecular orbital (HOMO), and the $\pi^*$

orbital is the lowest unoccupied molecular orbital (LUMO). The separation between

HOMO and LUMO is considered to be the band gap of organic electronic materials. The

band gap typically has a range of 1-4 electron volts (eV).[3]

R. N. Marks et al. created the first example of an OPV in 1994.[4] The single layer

device structure of this OPV cell was comprised of a transparent electrode/organic

photosensitive semiconductor/electrode.[3] He used a 50-320 nm thickness of poly(p-

phenylene vinylene) (PPV) sandwiched between indium tin oxide (ITO) glass and a low

work function cathode.[3] A work function is the minimum energy needed to remove an

electron from a solid, usually a metal, to a point immediately outside the solid surface.[3]

The reported quantum efficiencies for this device were around 0.1% when subjected to a

light intensity of 0.1 mW/cm$^2$.[3] Although the efficiency was low, this allowed for the

advancement of polymer based OPVs.

The discovery of conducting polymers and the ability to dope these polymers over

a broad range of materials—from insulators to metals—has resulted in the creation of a

new class of materials. These materials combine the electronic and optical properties of

semiconductors and metals, along with the attractive mechanical properties and

processing advantages of polymers. Moreover, the ability to control the energy gap and

electronegativity through molecular design has made it possible to synthesize conducting

polymers with a range of ionization potentials and electron affinities. The extended $\pi$-

orbitals of conjugated polymers result in a quasi-one-dimensional electronic structure

with associated novel nonlinear excitations.[5]

When these materials absorb a photon, an excited state is generated and confined to a molecule or a region of a polymer chain.[6] The excited state can be regarded as an electron-hole pair bound together by a Coulombic force forming an electrically neutral quasiparticle called an excition.[6] In OPVs, excitons are broken up into free electrons-hole pairs by effective fields. Forming a heterojunction between two dissimilar materials sets up the effective fields. A heterojunction is the boundary between two different semiconductor materials, usually with a negligible discontinuity in the crystal structure.[7] From here, effective fields divide excitons by causing the electron to fall from the conduction band of the electron donor to the conduction band of the electron acceptor. It is necessary that the acceptor material have a conduction band edge that is lower than that of the donor material.[8 - 9]

**Different Types of OPVs**

The simplest organic photovoltaic cell is the single layer OPV. It takes the most basic form of various OPVs. The cell is made up of three components, indium tin oxide (ITO) coated glass [electrode 1], the organic electronic material, and a layer of aluminum, magnesium, or calcium [electrode 2]. They are typically arranged by having the high work function metal on top (ITO), followed the organic electronic material in the middle and a layer of the low work function metal (Al, Mg, or Ca) on the bottom.[10] This structure can be seen in Figure 1.1.
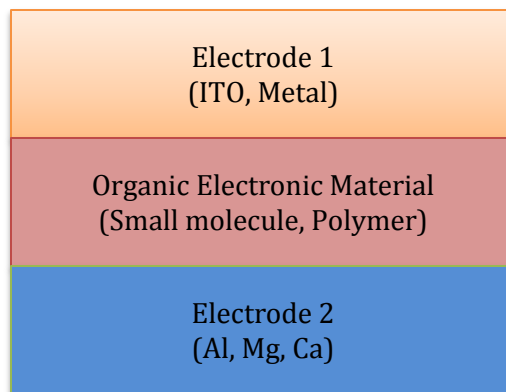
Figure 1.1: The schematic diagram of the single layer organic photovoltaic cell.

The difference of the work function between the two conducting electrodes creates an electric field in the organic electronic material. When the active organic layer is struck by a photon, the material absorbs it. Electrons in the material will be excited to LUMO, leaving a hole in the HOMO forming excitons. When the exciton falls from the excited state to the ground state, the electron-hole pair dissociates.[11] A hole is the conceptual and mathematical description for the lack of an electron where one could exist. The potential created by the different work functions helps to separate the exciton pairs, drawing electrons to the positive electrode and holes to the negative electrode. The current and voltage that are generated from completing this process can then be used to perform work. Heterojunction—based cells that rely on effective fields are more efficient than cells that rely on electric fields.[11]

The results of the single layer OPV show that they have low quantum efficiencies (<1%) and low power conversion efficiencies (<0.1%).[10] A major problem with this configuration is the electric field created from the difference between the two conductive

electrodes is rarely sufficient to divide the photogenerated excitons. As a result, the electrons recombine with the holes before they are able to reach their intended electrode.

To improve upon the single layer OPV, a second organic electronic layer could be added in conjunction with the first organic layer. This would create a bilayer OPV as shown in Figure 1.2.
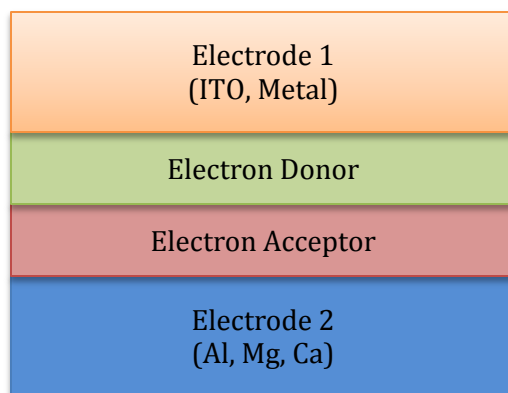


Figure 1.2: Device configuration of a bilayer organic photovoltaic cell.

This cell uses the same electrodes, but utilizes the differences between the two organic materials by taking advantage of the electron affinities and ionization energies. The layer with higher electron affinity and ionization potential is the electron acceptor, and the second layer is the electron donor. This generates electrostatic forces at the boundary between the two layers. The materials for the bilayer OPV must be chosen so that the properties of the materials have unequal band gaps to generate an electric field strong enough to divide excitons more efficiently than in the single layer OPVs.[6]

The diffusion length of excitons is the average length a carrier moves between division and recombination. In organic electronic materials this is typically on the order of 3 - 40 nm.[12] In order for most of the excitons to diffuse to the interface of the polymer

layers and disperse into charge carriers, the thickness of the polymer should be ~~also~~

within the same range of the diffusion length.  However, the typical polymer layer needs

to be at least 100 nm thick in order to absorb enough light.[6] At such a large thickness,

only a small fraction of the excitons can reach the heterojunction interface.

The polymer thickness and the small diffusion length of the excitions need to be

optimized to improve the efficiency of the bilayer OPV.  This can be achieved by

combining the electron donor and acceptor, forming a polymer blend, shown in Figure

1.3, called a dispersed (bulk) heterojunction.
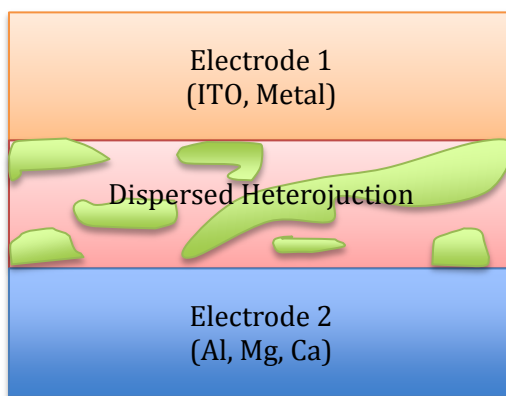


Figure 1.3: Device configuration of a bulk heterojunction organic photovoltaic cell.

This allows for the polymer blend length to become similar to the exciton

diffusion length.  This would allow the excitons generated in either material to reach the

interface where excitons can break efficiently.  This heterojunction has an increased

efficiency compared to the bilayer OPV by about 3% shown from experiments of Halls et

al. and Yu G. et al.[13-14] The slight disadvantage to this OPV configuration is the

consequence of electrons or holes becoming trapped in specific 'islands' active layer

without making their way to the electrode.  This creates the absence of an electron, or the

absence of a hole, in the material that needs to be filled by the next exciton that diffuses in range of this 'island'. This slows down the charge separation leading to lower device efficiencies.

Several advances have been made to improve upon the design of the electron donor and acceptor layers to make the OPV more efficient.[15-16] One example of this improvement is the graded heterojunction OPV. In this case the cell similar to bulk heterojunction, but the layering is gradual. The graded heterojunction uses the advantages of the bulk heterojunction, the short electron travel distance, and the bilayer, with its advantage of the charge gradient.[17] Another example is the controlled growth heterojunction. This provides better control over positions of the donor-acceptor materials, resulting in much higher power conversion efficiency than the bulk heterojunction.[18]

## II. Improving Organic Photovoltaic Performance

*Performance Measures, Factors, and Equations*

Organic photovoltaic cells are relatively cheap and cost effective. The power conversion efficiency (PCE) is the performance measure of OPVs denoted with $\eta$, which measures the amount of energy converted to electric current relative to the total energy incident upon the cell.[19] The PCE of improved organic photovoltaic cells must be higher than the current power conversion efficiency of OPVs, which has been reported to be ~8%.[15] A PCE of at least 10% must be achieved before OPVs can be considered viable and produced commercially.[19]

In order to achieve a PCE of 10% or more, three parameters must be manipulated:

absorption, charge separation, and charge transport.  Absorption is the percentage of light

that is absorbed by the active layer.  This is primarily affected by the band-gap and

thickness of the polymer, but it is also affected by the absorption in other layers,

reflection off the cell, and scattering within the cell.  Charge separation occurs when

excitons are created; electrons and holes must be separated from each other to prevent

recombination and the loss of energy in the form of light or heat. Charge separation is

influenced by the energy levels of the n-type and p-type semiconductor materials.  N-type

materials are capable of providing an extra electron to the host material and p-type

materials are capable of accepting an electron from the host material.  The morphology of

the active layer also plays a significant role.[20]  Since excitons can only diffuse a short

distance, the morphology must be such that there is an n/p interface within that short

distance for charge separation to occur successfully.[21] Charge transport occurs when

charge carriers are separated within the active layer.  They must be transported out of the

active layer to the circuit contacts. The effectiveness of this process is determined by the

mobility of these materials (that determines how effectively charge can be propagate

through them), and by the ability of a charge to find a contiguous path from its current

location to the appropriate electrode (i.e. anode for electrons and cathode for holes).

The formula for calculating PCE is

$$h = \frac{J_{sc}V_{oc}FF}{P_{in}}$$

where $\mathbf{J_{sc}}$ is the short-circuit current density (when maximum current is flowing and there

is no voltage difference across the circuit), $\mathbf{V_{oc}}$ is the open-circuit voltage (when there is

no current flowing - a break in the circuit), and $\mathbf{FF}$ is the fill-factor (the actual power

relative to the theoretical power produced by the cell). $\mathbf{P_{in}}$ is the incident solar radiation. This value is generally fixed at 100 mW/cm$^2$ when used in a solar simulator. The solar radiation on the ground is about 1000 W/m$^2$.[22]

By improving these three components, the power conversion efficiency of OPV cells can be improved. $\mathbf{J_{sc}}$ is largely affected by the band-gap, carrier mobility, and film formation properties of the active layer. $\mathbf{V_{oc}}$ is primarily affected by the material band-gap and the device structure, can be improved upon directly by optimizing the film layering, as seen in the bulk heterojunction, and device construction and design.[23] The last component, $\mathbf{FF}$, is particularly difficult to predict and design, because the relative mobilities of the electrons and holes can be difficult to predict depending upon the separation efficiency of the active layer.

**Incorporation of P3HT in OPVs**

Finding an active layer that will separate the excitons efficiently is a major component of the device design. There are several different active layers that have been used with one chemical species, as well as a ratio of multiple polymer species. Some of the polymer species that are currently being used are Buckminsterfullerene ($C_{60}$), [6,6]-phenyl-$C_{61}$-butyric acid methyl ester (PCBM), poly[2-methoxy-5-(2'-ethylhexyloxy)-p-phenylene vinylene] (MEH-PPV), poly[2-methoxy-5-(3'-7'-dimethyloctyloxy)-1,4-phenylenevinylene] (MDMO-PPV), and poly(3-octylthiophene) (P3OT).[22]

Poly(3-hexylthiophene) (P3HT) exhibits very promising results for its ability to be used as an active layer. This polymer gained its noteworthy status in 2000, when Alan Heeger, Alan MacDiarmid, and Hideki Shirakawa were awarded the Nobel Prize in

Chemistry for "the discovery and development of conductive polymers." The most notable property of these materials is their electrical conductivity.  This results from the delocalization of electrons along the polymer backbone yielding the term "synthetic metals".

Through my research with poly(3-hexylthiophenes), the results have shown an unprecedented PCE of about 3.8% using a 1:2 ratio of P3HT–functionalized nanoparticles:PCBM. The advantage of these 3-dimensional nanoparticles over bulk P3HT introduced by Krebs group[24] is allowing for self-assembly in the device and avoiding unordered assembly and broken-conjugated networks which can lower the power conversion efficiency of photovoltaic cells.  The PCE reported for their device using bulk P3HT was 0.3%, which was almost a thirteen-fold decrease.[24]

In my work, the synthesis method was developed to create functionalized spherical nanoparticles with a silicon-oxygen network using the modified Stöber method.[25] These networks are used for guiding the nanoparticles into ordered groups and create conjugated networks that would allow for the flow of electrons from the active layer to the opposite electrodes. The research of these findings has been submitted to the Journal of Chemistry of Materials.

CHAPTER 2

RESEARCH OBJECTIVE AND PROJECT GOALS

Objective:

To create functionalized nanoparticles derived from poly(3-hexylthiophene) as active

ligands for organic photovoltaic cells.  Two methods are used to create polythiophene

functionalized silonxane nanoparticles; the "grafting to" method using the modified

Stöber Method and the "grafting from" method using Grignard Metathesis.[26]

Goals:

- Preparation of P3HT-functionalozed siloxane nanoparticles using:

    o Method 1: "Grafting To" Method by the modified Stöber Method

    o Method 2: "Grafting From" Method by Grignard Metathesis

- Characterization and photophysical properties

- Photovoltaic performance

**Method and Approach**

The Stöber Method is a synthesis method for creating silica nanoparticles.[25] The

method uses a solution of ammonium hydroxide and absolute ethanol followed by the

drop wise addition of the precursor tetraethoxysilane.  The synthesis can proceed for 3-30

hours through hydrolysis-condensation reactions, leading to the formation of a spherical

nanoparticles that have a network of Si-O-Si bonds with hydroxyl functional groups on the surface. The modified Stöber Method uses the same process, but with the addition of a second precursor that contains organo-triethoxysilane group.[27] The second precursor is incorporated in the formation of the Si-O-Si network of the nanoparticle.

The advantages of using the modified Stöber method, over the regular Stöber method, are the functionalized precursor is directly incorporated into both the peripheral and core of the nanoparticle instead of functionalizing the nanoparticle through other experimental processes. There are a higher number of functionalized ligands directly incorporated into the nanoparticle, inside and out, instead of attaching ligands only to the surface of the silica nanoparticles.[27]

CHAPTER 3

EXPERIMENTAL METHODS

*Materials.* 2,5-dibromo-3-hexylthiophene, 5-bromo-2-thiophene carboxylic acid, tert-butylmagnesium chloride [$^t$BuMgCl] (1.6 M in THF), 2-hydroxyethylacrylate, 4-dimethyl amino pyridine (DMAP), N,N'-dicyclohexylcarbodiimide (DCC), chloroplatinic acid hexahydrate, dichloromethane (DCM), and anhydrous tetrahydrofuran were obtained from Aldrich chemicals. Ammonium hydroxide (28%) was obtained from Fischer Scientific. Triethoxysilane, tetraethoxysilane, dichloro[bis(1,3-diphenylphosphino)propane] nickel(II) [$Ni(dppp)_2Cl_2$] and 3-aminopropyltriethoxysilane were purchased from Alfar Aesar and used as received. Unless otherwise specified, all chemicals were used as received.

*Characterization.* Proton NMR spectra were recorded on a 500 MHz Jeol using chloroform-d ($CDCl_3$) as the solvent. FTIR spectra were measured using a Perkin-Elmer Spectrum One FT-IR spectrometer equipped with a universal ATR sampling accessory. Elemental analysis was conducted at the Advanced Materials Institute at Western Kentucky University. Transmission electron microscopy (TEM) observations were performed on a 100CX JEOL at 80 keV. Thermogravimetric analysis was performed at Thermal Analysis Laboratory at Western Kentucky University. The samples were

14

analyzed by a TA Q5000TGA. The samples were held isothermally at room temperature

for 30 min and then heated from room temperature to 650°C at 10°C/min in nitrogen. The

purge gas was heated at 10°C/min to 800°C. The photophysical properties in solution

were performed on fluorescence spectrometer (Perkin Elemer LS 55) and UV-visible

spectrometer (Perkin Elemer, Lambda 35).

*General procedure for the preparation of poly(3-hexylthiophene) (P3HT)*

2, 5-dibromo-3-hexylthiophene (5.000 g, 15.332 mmol) was added to a three-neck round

bottom flask and sealed with a water-jacket condenser and septum. The flask was

flushed with argon and anhydrous THF (30 mL) was injected. $^t$BuMgCl (15.33 mL,

15.33 mmol) was injected slowly and drop wise. This mixture was raised to 80°C using

an oil bath and refluxed for 2 hours under an argon atmosphere resulting in a yellow

solution. This solution was then cooled to room temperature and Ni(dppp)Cl$_2$ (0.138 g,

0.255 mmol) was added at once and the flask was flushed with argon. The reaction

continued for 30 minutes. The reaction turned blood red. Then Ni(dppp)Cl$_2$ (0.069 g,

0.128 mmol) was added again and continued for another 30 minutes. The reaction was

then quenched with 5 drops of methanol and precipitated in methanol (50 mL). The

purple precipitate was filtered out using a Büchner funnel and washed with hexane until

the filtrate became clear. Then the purple solid was dried under vacuum oven to yield

1.90 g of P3HT (Yield = 38.0%).

*Carboxylic acid terminated poly(3-hexylthiophene), 3*

Poly(3-hexylthiophene) (1.140 g, 0.950 mmol) was added to a three-neck round bottom
flask and sealed with a water-jacket condenser and septum. The flask was flushed with
argon and anhydrous THF (30 mL) was injected. $^{t}$BuMgCl (1.6 mL, 1.627 mmol) was
injected slowly and drop wise over a 70 minute period. This mixture was raised to 80°C
using an oil bath and refluxed for 2 hours under an argon atmosphere resulting in a
yellow solution. This solution was then cooled to room temperature and Ni(dppp)Cl$_2$
(0.013 g, 0.024 mmol) was added at once and the flask was flushed with argon. Then a
dry solution of 5-bromo-2-thiophene carboxylic acid (0.337 g, 1.627 mmol) in anhydrous
THF (5 mL) was injected into the flask and stirred for 45 minutes at room temperature
resulting in a purple mixture. The reaction was quenched with methanol (3 mL) and
precipitated in methanol (50 mL). The precipitate was filtered out using a Büchner
funnel. The resulting purple solid was dried thoroughly using a vacuum oven at room
temperature (1.535 g, Yield = 78.2%). $^1$H-NMR in CDCl$_3$ {$\delta$, ppm}: 7.44 (s (weak, br),
1H), 7.29 (s, (weak, br), 1H), 6.97 (s, 97H), 6.82(s (weak), 1H, terminal H), 2.80 (s (br),
180H), 1.77-1.34 (m, 900H), 0.91 (s, 323H); FT-IR stretchings (cm$^{-1}$): 3354-3000 (-OH
from carboxylic acid), 2921- 2854 (alkyl C-H), 1694 (carbonyl, weak), 1604-1509
(aromatic C-C), 1449 and 819 (S-C). Molecular weight (MW) of the polymer was
determined by $^1$H-NMR spectrum with respect to terminal hydrogen of P3HT polymer
chain end; MW = 16,200 g/mol.


*Carboxyethylacrylate chain end-functionalized P3HT, 4:* Carboxylic acid-terminated
P3HT {poly(3-hexylthiophene) with 2-thiophene carboxylic acid endcap} (1.04 g, 0.175

mmol), 2-hydroxyethyl acrylate (0.120 mL, 1.049 mmol), DCC (0.345 g, 1.673 mmol), and a catalytic amount of DMAP (0.015 g) were combined in a single-necked round bottom flask and flushed with argon.  Anhydrous THF (30 mL) was then injected creating a purple solution and the reaction stirred for 16 hours at room temperature under an inert gas atmosphere.  The reaction was then quenched with methanol (3 mL) and precipitated in methanol (50 mL).  The mixture was filtered using a Büchner funnel and washed with hexane until a clear was observed going into the filtrate.  The resulting dark purple solid thoroughly dried in a vacuum oven (1.400 g, Yield = 87.6%). $^{1}$H-NMR in CDCl$_3$ {$\delta$, ppm}: 7.44 (s (weak, br), 1H), 7.28 (s, (weak, br), 1H), 6.97 (s, 105H), 6.82(s (weak), 1H, terminal H), 2.79 (s (br), 211H), 1.69-1.33 (m, 1000H), 0.94 (s, 381H); FT-IR stretchings (cm$^{-1}$): 2922- 2854 (alkyl C-H), 1694 (carbonyl, weak), 1604-1511 (aromatic C-C), 1449 and 820 (S-C).

***Poly(3-hexylthiophene) carboxy triethoxysilane, (P3HT-acrylate silane precursor), 5:***
Poly(3-hexylthiophene) carboxy acrylate (0.700 g) was added into a three-neck round bottom flask and sealed with septum.  The flask was flushed with argon and anhydrous THF (30 mL) was injected.  Triethoxysilane (0.120 mL, 0.672 mmol) was slowly injected drop wise into the flask.  A dry 2 mol% solution of chloroplatinic acid hexahydrate (0.104 g, 0.200 mmol) in anhydrous ethanol (10 mL) was slowly added to the reaction vessel.  The reaction stirred for 16 hours at room temperature under an inert gas atmosphere.  The solution was quenched with methanol (5 mL) resulting in a purple precipitate and solution mixture.  The solution was further precipitated out using methanol (50 mL).  This liquid-solid mixture was filtered using a Büchner funnel and

washed with hexane until a clear was observed going into the filtrate.  The resulting solid

was dark purple and thoroughly dried in a vacuum oven (0.770 g, Yield = 84.25%).  $^{1}$H-

NMR in CDCl$_3$ {$\delta$, ppm}: 7.43 (s,weak, br, 1H), 7.29 (s, (weak, br), 1H), 6.97 (s, 92H),

6.82(s (weak), 1H, terminal H), 3.64 (s, weak, 3H), 2.80 (s (br), 188H), 1.80-1.34 (m,

997H), 0.91 (s, 331H); FT-IR stretchings (cm$^{-1}$): 3368 (OH from trace amount of

methanol wash), 2922- 2855 (alkyl C-H), 1696 (ester carbonyl from acrylate), 1636-

1512 (aromatic C-C), 1452 and 817 (S-C), 1157 (Si-C), 1068 (Si-O-) and 815.86.


***General procedure for the preparation of P3HT-Acrylate-SSQ nanoparticles, 6:***

Anhydrous ethanol (200 proof, 20 mL), ammonium hydroxide (28%, 5 mL), and

tetraethoxysilane (0.098 g, 0.47 mmol) were added at once into a one-necked round

bottom flask resulting in a clear solution.  This solution was allowed to stir until a milky,

white color appeared.  A previously prepared solution (by sonication) of poly(3-

hexylthiophene) carboxy acrylate triethoxysilane (0.100 g) and anhydrous THF (5 mL)

was added at once into the reaction vessel turning the solution color dark purple.  The

reaction was continued for 20 hours.  The solution was centrifuged yielding a clear,

colorless supernatant and a purple precipitate.  The supernatant was decanted and saved.

The precipitate was allowed to dry in the fume hood until a purple powder was observed.

The procedure resulted in 260 nm average size particles confirmed by TEM. FT-IR

stretchings (cm$^{-1}$): 3243 (OH from hydrolyzed silanol groups), 2923-2855 (alkyl C-H),

1696 (ester carbonyl from acrylate), 1636-1512 (aromatic C-C), 1437 and 813 (S-C),

1040 (Si-O-Si).

***2-Bromo-3-thiophene carboxyacrylate:*** 2-Bromo-3-thiophene carboxylic acid (2.508 g, 12.114 mmol), 2-hydroxyethyl acrylate (1.39 mL, 12.077 mmol), DCC (3.739 g, 18.121 mmol), DMAP (19 mg), were combined into a three-neck round bottom flask, sealed with an adapter for argon flow and septum,-and flushed with argon.  Anhydrous THF (50 mL) was then injected into the flask resulting in a milky, white solution.  The reaction was continued overnight (10-12 hours).  The resulted white precipitate was filtered.  The clear solution was mixed with 70 mL of deionized ice water and transferred into a separatory funnel.  DCM (15 mL) was added to the funnel and inverted.  Two phases appeared and the bottom DCM phase was removed.  This was performed until three extractions were completed.  The extractions were collected together and concentrated under vacuum to minimum volume using a rotovap.  The clear solution became a yellowish oil upon concentration where it later solidified at room temperature. $^1$H-NMR in $CDCl_3$ {$\delta$, ppm}: 7.35-7.26 (d, 1H), 6.46-6.43 (d, 1H), 6.18-6.11 (dd, 1H), 5.88-5.85(d, 1H), 4.31-4.29 (t, 4H).

***2-Bromo-3-thiophene carboxyacrylate silane precursor:*** 2-bromo-3-thiophene carboxyacrylate (1.00 g, 3.277 mmol) was added to a one-neck round bottom flask and flushed with argon.  Anhydrous THF (30 mL) was injected and the mixture was allowed to stir for 5 minutes until it dissolved.  A dry solution of 2.0-mol% chloroplatinic acid hexahydrate (0.104 g, 0.200 mmol) in anhydrous ethanol (10 mL) slowly added (or injected) drop wise to the reaction vessel.  15 minutes after the solution was added triethoxysilane (0.80 mL, 3.604 mmol) was added (or injected) slowly to the reaction vessel.  The reaction was continued for 16 hours resulting in a cloudy, milky yellow

color. The reaction was quenched with methanol (5 mL) precipitated methanol (50 mL) was used for precipitating the product. No precipitation occurred with the addition of methanol. The solution was concentrated under vacuum to minimum volume using a rotovap. The resulting solution solidified into a white-yellow powder. $^{1}$H-NMR in CDCl$_3$ {$\delta$, ppm}: 7.27-7.26 (d, 1H), 6.94-6.93 (d, 1H), 4.03-4.02 (q, 6H), 3.91- 3.88 (t, 2H), 3.53-3.52 (t, 2H), 2.03-2.01 (t, 2H), 1.19-1.18 (t, 9H).

***Thiophene Monomer Functionalized NP:*** Anhydrous ethanol (200 proof, 50 mL), ammonium hydroxide (28%, 3 mL), and tetraethoxysilane (0.098 g, 0.47 mmol) were added at once into a one-necked round bottom flask resulting in a clear solution. This solution was allowed to stir until a milky, white color appeared. A previously prepared solution (by sonication) of 2-bromo-3-thiophene carboxyacrylate triethoxysilane (0.100 g) and anhydrous THF (5 mL) was or injected at once into the reaction vessel. The reaction was continued for 20 hours. The cloudy, milky white solution was centrifuged yielding a clear, milky white supernatant and a white precipitate. The supernatant was decanted and saved. The precipitate was allowed to dry in the fume hood until a white powder was observed. Particle size distribution was examined under TEM yielding an average particle size of 90 – 99 nm.

***Grafting P3HT from Monomer Fucnctionalized Nanoparticle Surface:*** 2-Bromo-3-thiophene carboxyacrylate nanoparticle (0.024 g) was added to a three-neck round bottom flask and flushed with argon and sealed with a water-jacket condenser and septum. Anhydrous THF (10 mL) and tert-butylmagnesium chloride (0.33mL) were then injected

into the reaction vessel resulting in a clear yellow solution.  This mixture was raised to 80°C using an oil bath and refluxed for 2 hours under an argon atmosphere.  After 1 hour, 2,5-Dibromo-3-hexylthiophene (0.33 mL) was added to the reaction vessel and the reaction continued to reflux for an additional hour.  This solution was then cooled to room temperature and Ni(dppp)Cl$_2$ (0.002 g) was added at once.  The system was flushed with argon and stirred for 30 minutes.  An additional portion of Ni(dppp)Cl$_2$ (0.002 g) was added and stirred another 30 minutes.  This resulted a cloudy, peach colored solution.  The reaction was quenched with 5mL of methanol and then centrifuged.  The supernatant was saved and the precipitate was allowed to dry in the fume hood.  Grafted particles were characterized on the TEM shown in Figure 4.7.  FT-IR: stretchings (cm$^{-1}$): 3342 (OH from hydrolyzed silanol groups), 2924-2852 (alkyl C-H), 1634-1520 (aromatic C-C), 1436 and 845 (S-C), 1260 Si-C, 1180-1121 (Si-O-Si).

CHAPTER 4

RESULTS AND DISCUSSION


Poly(3-hexylthiophene)-functionalized silsesquioxane nanoparticles were produced through a series of experiments using two different approaches: a "grafting to" approach using a modified Stöber method and a "grafting from" approach using Grignard Metathesis.[16]

**I. Synthesis**

*Synthesis of P3HT-SSQ using the "grafting to" method:*

The initial molecule used for the "grafting to" method was 2,5-dibromo-3-hexylthiophene, which was used in a Grignard Metathesis/Kumada Coupling reaction to yield poly(3-hexylthiophene). This product was then end-capped with 5-bromo-2-thiophenecarboxylic acid in a Grignard Metathesis/Kumada Coupling reaction to yield poly(3-hexylthiophene) with the carboxylic acid group at the chain end. An esterification reaction was then performed using DCC coupling with 2-hydroxethylacrylate to create poly(3-hexylthiophene) carboxyacrylate. The product was used in hydrosilylation reaction to yield poly(3-hexylthiophene) carboxyacrylate triethoxysilane precursor. The condensation of the silane precursor using a modified Stöber method yield the desired final product of poly(3-hexylthiophene)- functionalized nanoparticles.
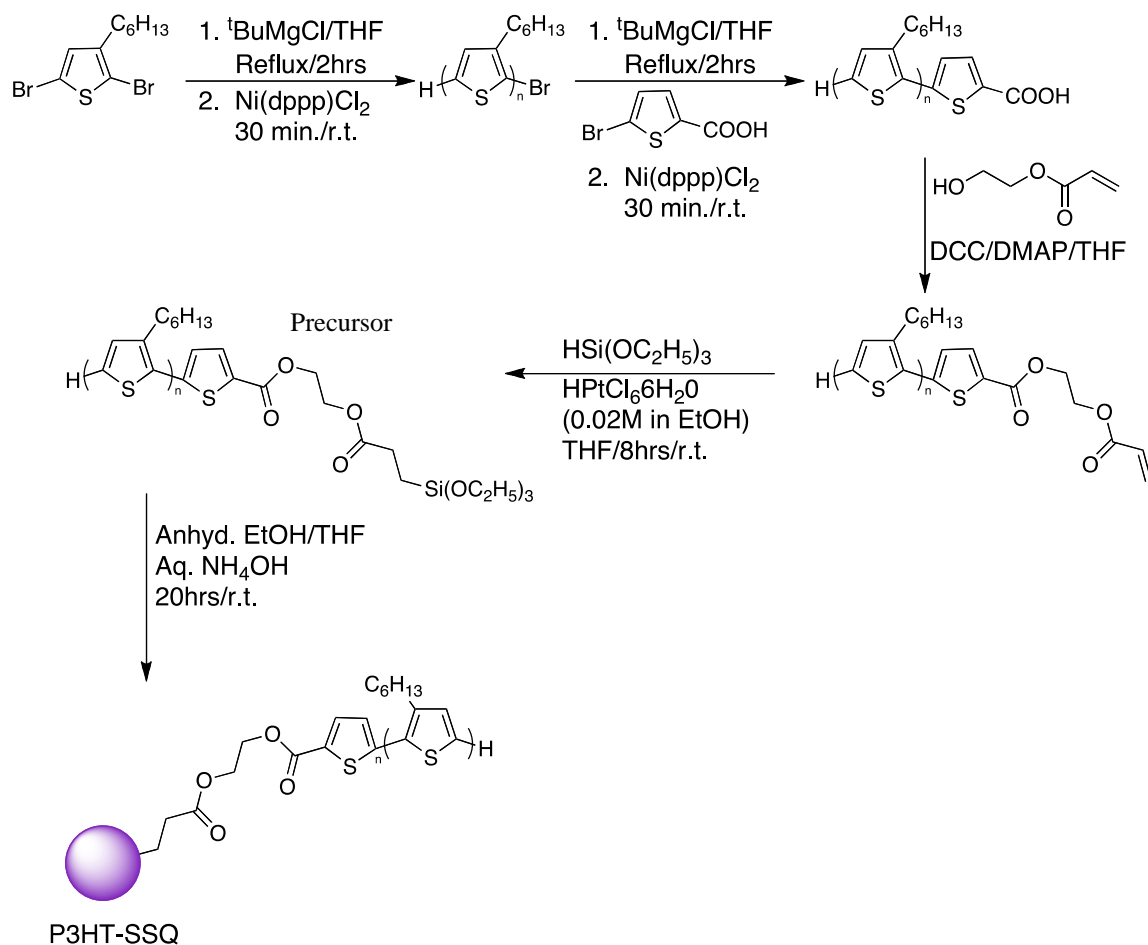
Scheme 4.1: Preparation of P3HT SSQ nanoparticles using the modified Stöber Method with the poly(3-hexylthiophene) carboxyacrylate triethoxysilane precursor.

Four trails were performed using the "grafting to" approach. Table 4.1 shows the experimental conditions and the particle size distribution.

Table 4.1: Experiment number and reaction conditions for creating P3HT nanoparticles.

| P3HT-NPs Trials | 28% $NH_4OH$ (mL) | Silane:TEOS | TEOS (mmol) | Particle Size Distribution (nm) | % Yield |
|---|---|---|---|---|---|
| 1 | 5 | 1:30 | 0.48 | 260 | 65% |
| 2 | 5 | 1:30 | 0.48 | 99 and 108 | 60% |
| 3 | 10 | 1:30 | 0.48 | 117 and 126 | 65% |
| 4 | 5 | 1:30 | 0.48 | 36-54 and 90 | 60% |

*P3HT Silane used for each trial = 0.016136 mmol.

23

As shown in the Table 4.1, a constant amount of P3HT Silane is used in all of these trails. Trail one shows the reaction conditions for the first trial of functionalized nanoparticles. Using a 4:1 ratio of ethanol (EtOH):tetrahydrofuran (THF) the reaction yield was about 65%. The transmission electron microscope (TEM) was confirmed the particle size distribution with an average particle size of 260 nm.

In trial two, all of the reaction conditions were kept constant and the EtOH:THF ratio was doubled. This resulted an averaged particle size of 104 nm particles, which was a substantial decease in particle size distribution from trail one.

Trial three maintained the same EtOH:THF ratio as trail two and doubled the concentration of ammonium hydroxide ($NH_4OH$). The observed yield increased to 65% and the average particle size increased by 18 nm. This increase in particle size is not favorable for light absorption as will be seen in the photophysical properties later.

Trial four was performed to see if a smaller particle size could be achieved. The reaction conditions for trial four went back to the basic conditions of trial one and tripled the EtOH:THF concentration. The reaction yield was about 60% and the average particle size by TEM analysis were between 36–54 nm and 90 nm.

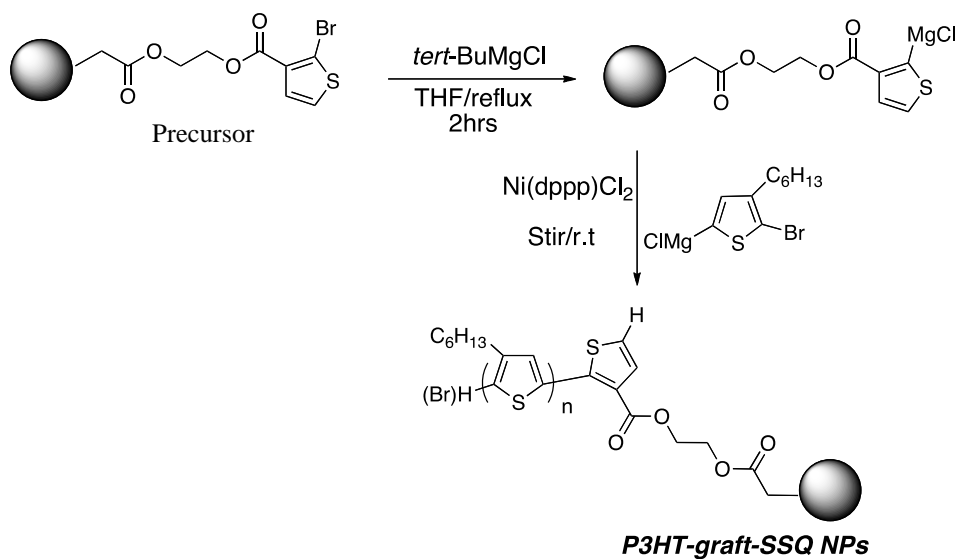*Synthesis of P3HT-SSQ using the "grafting from" method:*

In the "grafting from" method, the first step was creating a bromine functionalized silsesquioxane nanoparticles as an initiated monomer for the polymerization of 2,5-dibromo-3-hexylthiophene to yield P3HT-graft silsesquioxane nanopartilces. Starting from 2-bromo-3-thiophene carboxylic acid, 2-bromo-3-thiophene carboxyacrylate was prepared upon esterification with 2-hydroxethylacrylate in the

24

presence of DCC. Then the hydrosilylation reaction was carried out with triethoxysilane in the presence of platinum catalyst to yield 2-bromo-3-carboxyacrylate triethoxysilane precursor, which was used to create bromine functionalized silsesquioxane nanoparticles. These initiator functionalized nanoparticles were reacted with 2,5-dobromo-3-hexylthiophene using Grignard Metathesis to prepare P3HT-graft-nanoparticles in considerable good yield (Scheme 2). However, compare to "grafting to method", the surface functionalized grafting from method yield above 20% of free polymer (ungraft P3HT).

**(a). Preparation of surface-initiator functionalized NPs**

**Surface-initiator functionalized NPs**
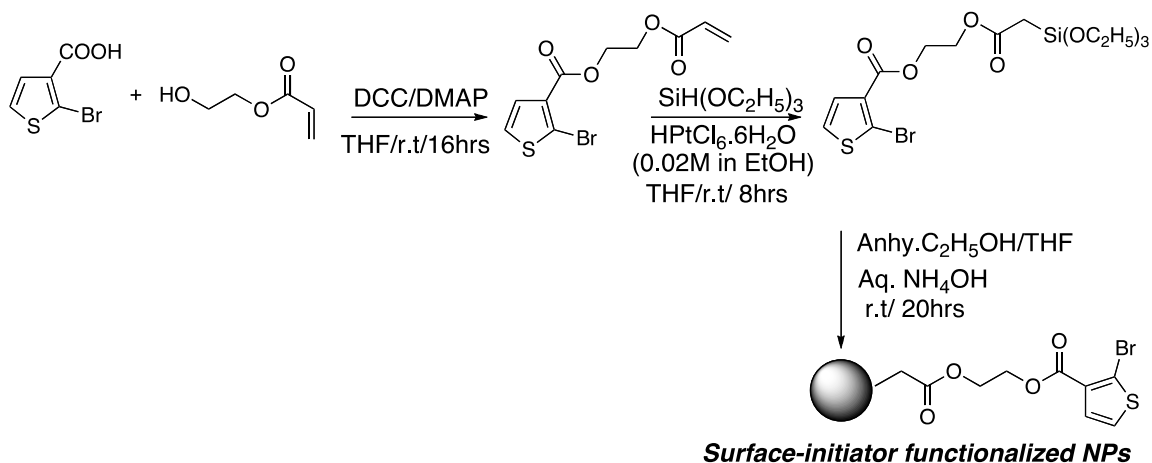
**(b). An Application of surface-initiated Grignard Metathesis**

Precursor

**P3HT-graft-SSQ NPs**

Scheme 4.2: Preparation of P3HT SSQ nanoparticles using Grignard Metathesis.

Three trails were performed using the "grafting from" approach. Table 4.2 shows the experimental conditions.

Table 4.2: Reaction conditions for creating P3HT nanoparticles.

| P3HT-NPs Trials | 28% NH$_4$OH (mL) | Silane:TEOS | TEOS (mmol) | Particle Size Distribution (nm) | % Yield |
|---|---|---|---|---|---|
| 1 | 3 | 1:2.2 | 0.48 | 90 – 99 | 12% |
| 2 | 3 | 1:2.2 | 0.48 | N/A | 15% |
| 3 | 6 | 1:2.2 | 0.96 | 63 – 130 | N/A |

*Thiophene Monomer Silane used for trials 1 and 2 = 0.21862 mmol.
*Thiophene Monomer Silane used for trail 3 = 0.43725 mmol

These trails correspond to the third experimental step in the reaction series where the modified Stöber method is used to create ungrafted nanoparticles. As shown in Table 4.2, a constant amount of thiophene monomer silane was used in trails 1-2 and it was doubled in trail three. Trail one shows the reaction conditions for the first trial of the thiophene monomer nanoparticles. Using a 10:1 ratio of EtOH:THF the reaction yield was about 12% and the average particle size observed using the TEM was 94 nm. The particles are of good size for incorporation into device fabrication, but a smaller and more uniform average size would be more desirable. Trail two is a reproduction of trail one to try and reproduce the results. A higher yield of 15% was achieved, but the average particle size could not be maintained at 94 nm.

All the reaction conditions were doubled in trail three while maintaining the solvent ratio of EtOH:THF of 10:1. The nanoparticles tend to stay in the solution rather than precipitation out from the solution. The TEM images revealed the particle size in the range of 63-130 nm. The particle size distribution was considerably wide.

27

## II. Characterization

As shown in Figure 4.1 and 4.2, TEM images were taken from trails 1 and 2? Not 4 to confirm the grafted P3HT on to nanoparticles.
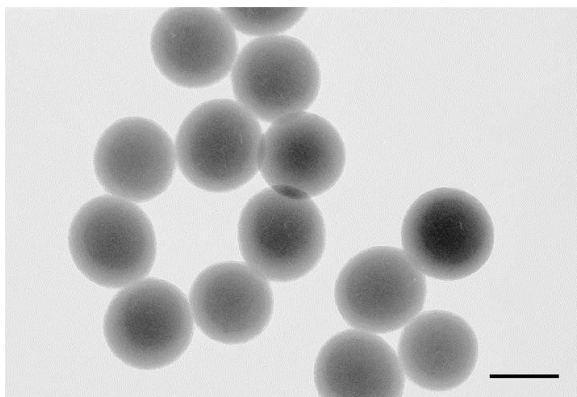


Figure 4.1: Trail 1
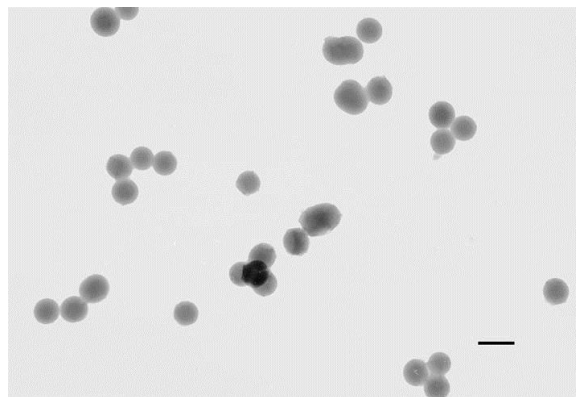P3HT-SSQ nanoparticles
(Scale bar 200 nm)

Figure 4.2: Trail 4
P3HT-SSQ nanoparticles
(Scale bar 100 nm)

The morphology of the nanoparticles is nearly a perfect sphere. The images show a zoomed in portion of a droplet of product, allowing the product to air-dry on a 200 nm mesh carbon coated grid first, where the spheres do not overlap, or overlap by much, and come into relatively close contact with one another. This is very useful information that can be used in device creation to begin to understand how the nanoparticles will interact with each other.

These polymer-graft nanoparticles were characterized by FT-IR spectroscopy and the spectrum is shown in Figure 4.3.
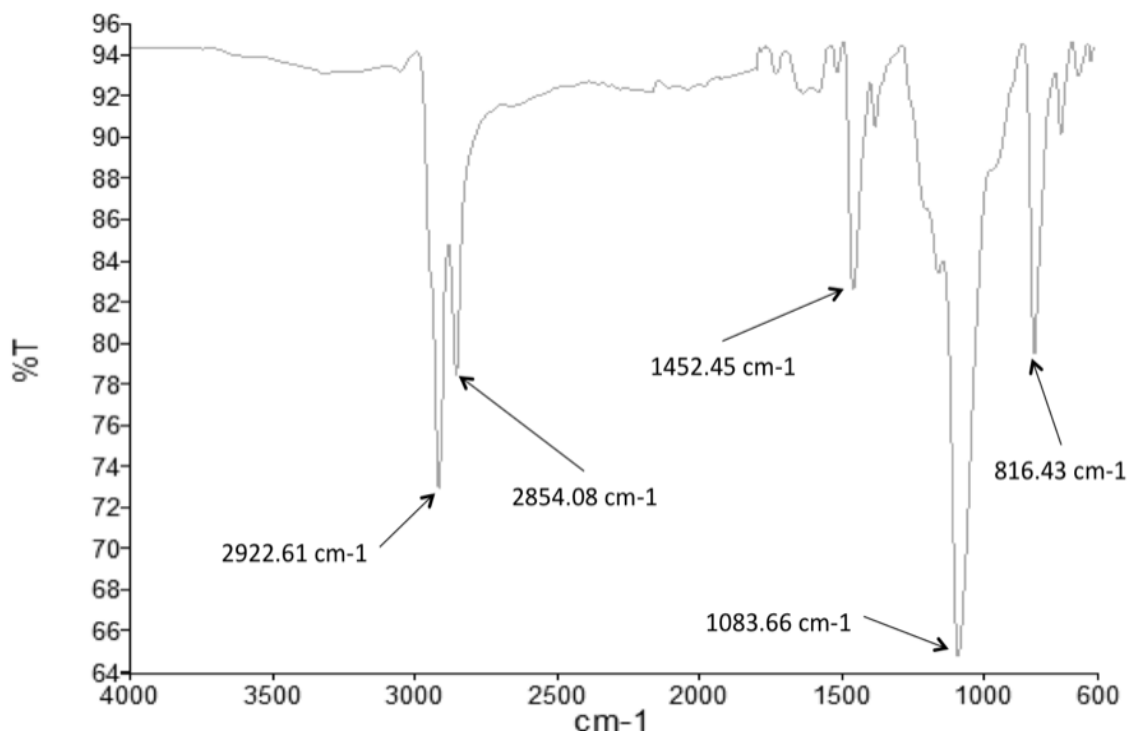
Figure 4.3: IR analysis of the "grafting to" P3HT-SSQ Nanoparticles.

The characteristic peak at 816.43 $cm^{-1}$ confirms an aromatic sulfur-carbon bond (S—C) of the thiophene ring. The peak at 1083.66 $cm^{-1}$ confirms the presence of silicon-oxygen network (Si—O—Si) from the nanoparticle core. The stretchings from aromatic carbon-carbon bonds of the thiophene rings at 1452.45 $cm^{-1}$ further supports the attachment of thiophenes to the nanoparticles. The alkyl stretching from hexyl linkers of thiophene rings can be found at 2854.08 $cm^{-1}$ - 2922.61 $cm^{-1}$.

The solution phase photophysical properties of these nanoparticles were studied to confirm the optical behavior of these polymer graft nanoparticles. Figure 4.4 shows the UV-visible spectra of two different sizes of P3HT-nanoparticles in chloroform solution. The nanoparticle with 50 nm sizes showed a broad absorption band with $\lambda_{max}$ at 445 nm, which agrees with the absorption spectra obtained for the P3HT-silane monomer

absorption.  The larger nanoparticles (350 nm) show a boarding and a slight shift of $\lambda_{max}$

at 445 nm.  This slight spectral boarding may be due to the different packing pattern of

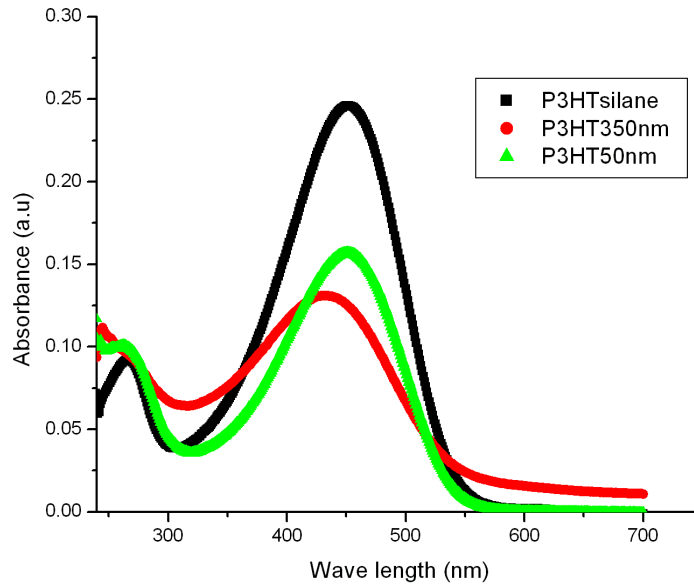the P3HT polymer chains in the siloxane matrix.[28]



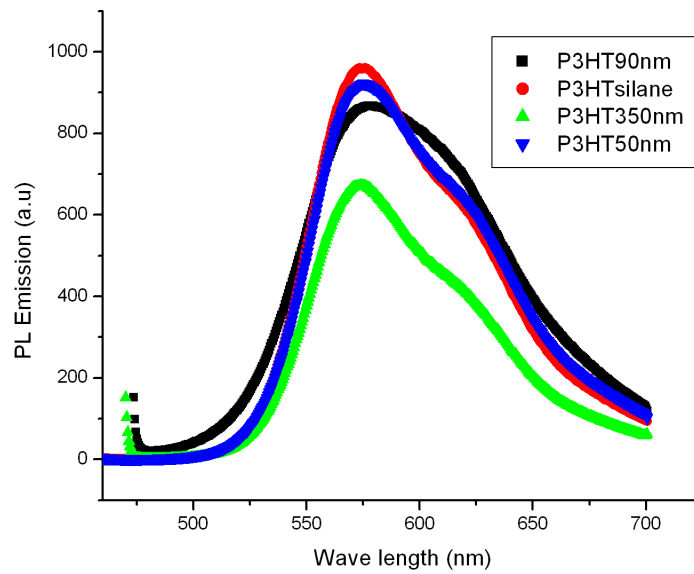Figure 4.4: UV-vis of P3HT-SSQ NPs in a chloroform solution.



Figure 4.5: Fluorescence emission spectra of P3HT-SSQ NPs in chloroform solution.

Figure 4.5 shows the photoluminescence (PL) behavior of polymer-functionalized nanoparticles in solution. The PL emission of P3HT-NPs in solution exhibits bright yellow fluorescence at 580 nm with a shoulder peak around 630 nm. This follows the spectral pattern of P3HT-silane precursor. The PL emission spectrum of the 90 nm P3HT-NPs does not follow this pattern however. This emission spectrum displays a broad peak around 580 nm.

For the "grafting from" method, the polymer graft nanoparticles were examined under TEM and shown in Figure 4.6-4.7.
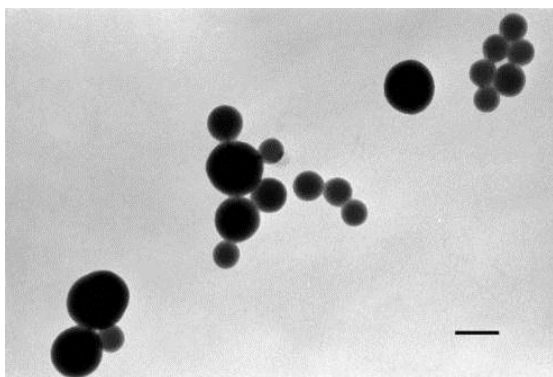


Figure 4.6: Trail 3
TEM image of bare nanoparticles
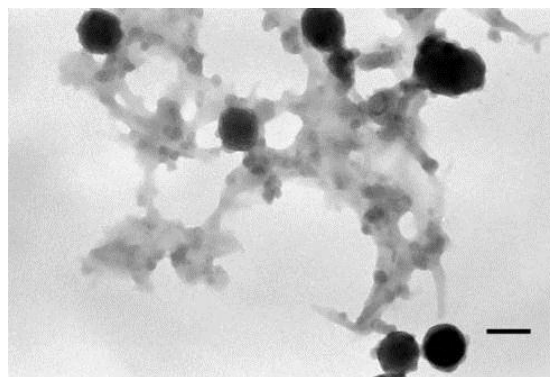
Procedure (a)
(Scale bar-100 nm)

Figure 4.7: Trial 3
TEM image of P3HT-graft-SSQ nanoparticles

Procedure (b)
(Scale bar-100 nm)

The morphology of polymer-grafted nanoparticles is clearly shows the polymer layer with uneven edges on the nanoparticle's surface. The "webbing" between the nanoparticles was free polymer resulted from typical Grignard metathesis. However, further characterization is needed to confirm the density of polymer-graft from nanoparticle's surface.

31

### III. Photovoltaic Performance

The photovoltaic performance of P3HT-functionalized nanoparticles obtained from "grafting to" method was evaluated using the following device configuration (Figure 4.8).

**P3HT-SSQ NPs/PCBM**
**(1:1)**

**Al**

**LiF**

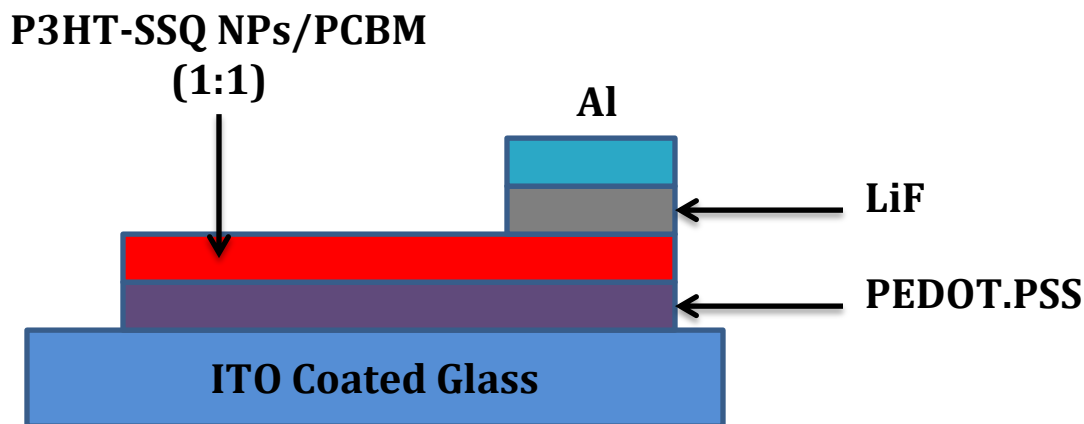**PEDOT.PSS**

**ITO Coated Glass**

Figure 4.8: The device components and layers of the OPV starting from the bottom. ITO/PEDOT.PSS/ Active layer/LiF-Al

Device Preparation:

Model bulk heterojunction solar cell devices were prepared on glass/ITO substrates. The substrates were subsequently cleaned in 2-propanol and acetone in ultrasonic bath for 10 minutes each and a thin layer of PEDOT:PSS (purchased from Aldrich) with a thickness of ~70-80 nm was spin coated as a hole transporting layer on top of ITO under nitrogen atmosphere. The substrates were heated at 100°C in a vacuum oven for an hour. As a first step, the active layer of P3HT-NPs:PCBM with 1:1 ratio dissolved in chlorobenzene (15 mg/mL concentration of each compound for the 1:1 blend) was spin coated at a rotational speed of 1000 rpm to give a film thickness of 80-100 nm. The casting of the active layer on the substrate was carried out inside a glove

box under nitrogen atmosphere. The substrates were transported into vacuum evaporator

and a layer of LiF (~4 nm) and Al (~200 nm) was thermally evaporated on top of the

active layer with a diameter of 2 x 6 mm of coating area through a mask. The final

devices were annealed inside the glove box at different temperatures for ten minutes

followed by transfered to a glass chamber under stream of nitrogen gas and sealed the

chamber for device characterization. The testing of the devices was performed using a

solar simulator with an emission spectrum close to AM 1.5G and intensity of 100

mW/m$^2$. The IV curves of the devices were measured using a Keithley 2400 sourcemeter

controlled by a PC.  The fill factor (FF) and power conversion efficiency (PCE) were

calculated manually using following two equations.

$$FF = \frac{J_m V_m}{J_{sc} V_{oc}} \quad PCE = \frac{J_{sc} V_{oc} FF}{P_{in}},$$ where P$_{in}$ is the intensity of light.
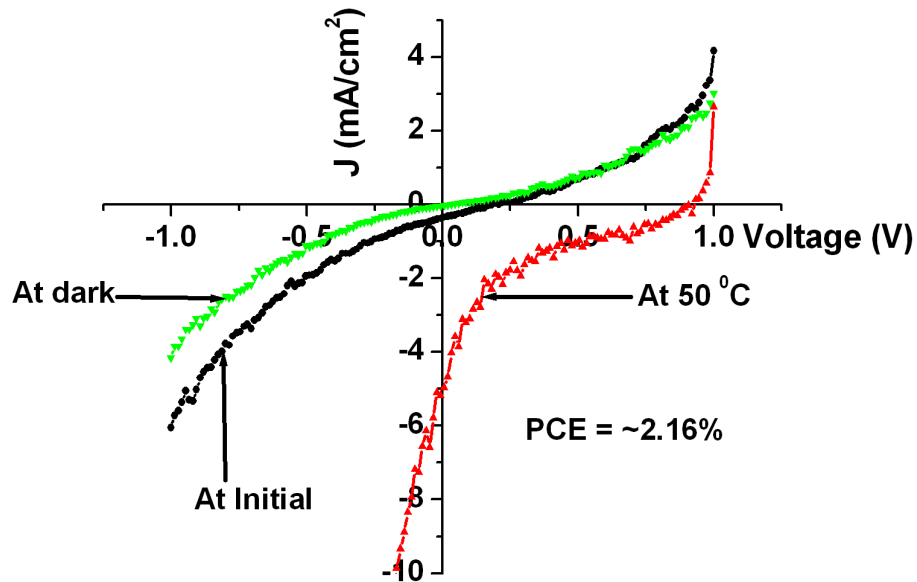
Device Characterization:



Figure 4.9: Current Density vs. Voltage with PCEs at dark, before annealing, and after annealing at 50˚C using voltages from -1.0 to 1.0 mV.

Using the device configuration shown in Figure 4.8, the P3HT-SSQ nanoparticles used were found to yield a PCE of about 2.16% with the best test device yielding a PCE of 2.46%. The $V_{OC}$ used in this performance test was found to be 0.83 V When comparing the performance of these nanoparticles to the P3HT-silica nanoparticles found in the literature[16], a PCE of 1.8—2.3% was reported. When comparing the PCE of the best test device from the lab compared to the best test device found from this literature source, a 3.36% increase in efficiency was seen. The $V_{OC}$ of this test device was found to be 0.60—0.62 V. This is a 0.23—0.21 V decrease from the best test device made in the lab.

CHAPTER 5

CONCLUSION

Two different types of novel fluorescent siloxane nanoparticles were successfully prepared using the modified Stöber Method and Grignard Metathesis. By varying the reaction conditions, different polymer-grafts nanoparticles were obtained. The morphology of these functionalized nanoparticles were examined using TEM. The particles were further characterized by IR, UV-Vis, and fluorescence spectroscopy. The photovoltaics performance of P3HT-nanoparticles was evaluated and we were able to improve the power conversion efficiency up to 2.16% with the device configuration of ITO/PEDOT:PSS/P3HT-NPs:PCBM/LiF/Al. The device efficiency obtained for P3HT-graft nanoparticles is about two-folds higher than the P3HT-functionalized hairy silica nanoparticles published recently.[16] The future work of this project will focus on optimizing the conditions to achieve higher power conversion of ~5%, which will be compete with the commercially available organic- based photovoltaic devices.

REFERENCES

[1] Serway, R. A., *Physics for scientists & engineers*. Saunders College Pub.: 1990.

[2] Lewis, N. S., Toward Cost-Effective Solar Energy Use. *Science* **2007,** *315* (5813), 798-801.

[3] Rivers, P. N., *Leading edge research in solar energy*. Nova Science Publishers: 2007.

[4] Marks, R. N.; Halls, J. J. M.; Bradley, D. D. C.; Friend, R. H.; Holmes, A. B., The photovoltaic response in poly(p-phenylene vinylene) thin-film devices. *Journal of Physics: Condensed Matter* **1994,** *6* (7), 1379.

[5] Sariciftci, N. S.; Smilowitz, L.; Heeger, A. J.; Wudl, F., Photoinduced Electron Transfer from a Conducting Polymer to Buckminsterfullerene. *Science* **1992,** *258* (5087), 1474-1476.

[6] Schnabel, W., *Polymers and Light: Fundamentals and Technical Applications*. John Wiley & Sons: 2007.

[7] Winder, C.; Sariciftci, N. S., Low bandgap polymers for photon harvesting in bulk heterojunction solar cells. *Journal of Materials Chemistry* **2004,** *14* (7), 1077-1086.

[8] McGehee, M. D.; Topinka, M. A., Solar cells: Pictures from the blended zone. *Nat Mater* **2006,** *5* (9), 675-676.

[9] Hoppe, H.; Sariciftci, N. S., Organic solar cells: An overview. *Journal of Materials Research* **2004,** *19* (7), 1924-1945.

[10] Kim, M. S.; Michigan, U. o., *Understanding Organic Photovoltaic Cells: Electrode, Nanostructure, Reliability, and Performance*. University of Michigan: 2009.

[11] Hoppe, H.; Sariciftci, N. S., Morphology of polymer/fullerene bulk heterojunction solar cells. *Journal of Materials Chemistry* **2006,** *16* (1), 45-61.

[12] Yam, V. W. W., *WOLEDs and Organic Photovoltaics: Recent Advances and Application*. Springer: 2010.

[13] Halls, J. J. M.; Pichler, K.; Friend, R. H.; Moratti, S. C.; Holmes, A. B., Exciton diffusion and dissociation in a poly(p-phenylenevinylene)/C[sub 60] heterojunction photovoltaic cell. *Applied Physics Letters* **1996,** *68* (22), 3120-3122.

[14] Yu, G.; Gao, J.; Hummelen, J. C.; Wudl, F.; Heeger, A. J., Polymer Photovoltaic Cells: Enhanced Efficiencies via a Network of Internal Donor-Acceptor Heterojunctions. *Science* **1995,** *270* (5243), 1789-1791.

[15] Thompson, B. C.; Fréchet, J. M. J., Polymer–Fullerene Composite Solar Cells. *Angewandte Chemie International Edition* **2008,** *47* (1), 58-77.

[16] Senkovskyy, V.; Tkachov, R.; Beryozkina, T.; Komber, H.; Oertel, U.; Horecha, M.; Bocharova, V.; Stamm, M.; Gevorgyan, S. A.; Krebs, F. C.; Kiriy, A., "Hairy" Poly(3-hexylthiophene) Particles Prepared via Surface-Initiated Kumada Catalyst-Transfer Polycondensation. *Journal of the American Chemical Society* **2009,** *131* (45), 16445-16453.

[17] Pandey, R.; Holmes, R. J., Graded Donor-Acceptor Heterojunctions for Efficient Organic Photovoltaic Cells. *Advanced Materials* **2010,** *22* (46), 5301-5305.

[18] Yang, F.; Shtein, M.; Forrest, S. R., Controlled growth of a molecular bulk heterojunction photovoltaic cell. *Nat Mater* **2005,** *4* (1), 37-41.

[19] Peters, C. H.; Sachs-Quintana, I. T.; Kastrop, J. P.; Beaupré, S.; Leclerc, M.; McGehee, M. D., High Efficiency Polymer Solar Cells with Long Operating Lifetimes. *Advanced Energy Materials* **2011,** *1* (4), 491-494.

[20] Miessler, G. L.; Tarr, D. A., *Inorganic chemistry*. Third ed.; Pearson Education: 2004.

[21] Lista, M.; Areephong, J.; Orentas, E.; Charbonnaz, P.; Sakai, N.; Matile, S., Engineering antiparallel charge-transfer cascades into supramolecular n/p-heterojunction photosystems: Toward directional self-sorting on surfaces. *Faraday Discussions* **2012,** *155* (0), 63-77.

[22] Benanti, T.; Venkataraman, D., Organic Solar Cells: An Overview Focusing on Active Layer Morphology. *Photosynthesis Research* **2006,** *87* (1), 73-81.

[23] Steim, R.; Kogler, F. R.; Brabec, C. J., Interface materials for organic solar cells. *Journal of Materials Chemistry* **2010,** *20* (13), 2499-2512.

[24] Krebs, F. C., All solution roll-to-roll processed polymer solar cells free from indium-tin-oxide and vacuum coating steps. *Organic Electronics* **2009,** *10* (5), 761-768.

[25] Stöber, W.; Fink, A.; Bohn, E., Controlled growth of monodisperse silica spheres in the micron size range. *Journal of Colloid and Interface Science* **1968,** *26* (1), 62-69.

[26] Loewe, R. S.; Khersonsky, S. M.; McCullough, R. D., A Simple Method to Prepare Head-to-Tail Coupled, Regioregular Poly(3-alkylthiophenes) Using Grignard Metathesis. *Advanced Materials* **1999,** *11* (3), 250-253.

[27] Arkhireeva, A.; Hay, J. N.; Oware, W., A versatile route to silsesquioxane nanoparticles from organically modified silane precursors. *Journal of Non-Crystalline Solids* **2005,** *351* (19-20), 1688-1695.

[28] Wright, N.; Patel, A.; Binion, J.; Scardino, D. J.; Hammer, N. I.; Rathnayake, H., "Poly(thiophene) functionalized ormosils for Organic based solar cells." *Chem. Mater.* **2012**. *Submitted.*